Analysis of quasi-brittle materials using two-dimensional polygon particle assemblies

Jong Seok Lee†

Department of Civil & Environmental Engineering, University of Ulsan, Ulsan, Korea

Yoon Bock Rhie‡

Rhie & Associates, Inc., 1900 N. Vine St. #407, Los Angeles, CA 90068, USA

Ick Hyun Kim‡†

Department of Civil & Environmental Engineering, University of Ulsan, Ulsan, Korea

Abstract.   This paper contains the results of the study on the development of fracture and crack propagation in quasi-brittle materials, such as concrete or rocks, using the Discrete Element Method (DEM). A new discrete element numerical model is proposed as the basis for analyzing the inelastic evolution and growth of cracks up to the point of gross material failure. The model is expected to predict the fracture behavior for the quasi-brittle material structure using the elementary aggregate level, the interaction between aggregate materials, and bond cementation. The algorithms generate normal and shear forces between two interfacing blocks and contains two kinds of contact logic, one for connected blocks and the other one for blocks that are not directly connected. The Mohr-Coulomb theory has been used for the fracture limit. In this algorithm the particles are moving based on the connected block logic until the forces increase up to the fracture limit. After passing the limit, the particles are governed by the discrete block logic. In setting up a discrete polygon element model, two dimensional polygons are used to investigate the response of an assembly of different shapes, sizes, and orientations with blocks subjected to simple applied loads. Several examples involving assemblies of particles are presented to show the behavior of the fracture and the failure process.

Key words: quasi-brittle materials; discrete element method; polygon block elements; Voronoi; failure.

1. Introduction

Quasi-brittle materials, such as concrete and rocks, are heterogeneous composite materials for which nonlinear behavior is caused by factors such as crushing, aggregate interlock, shrinkage and

---

† Professor
‡ Principal
‡† Assistant Professor

creep. There have been many researchers studying the inelastic behavior of quasi-brittle materials, especially for concrete and rocks, in the structural mechanics field. In their studies, materials are viewed as a homogeneous even though they are inhomogeneous. Most of them, however, are primarily based on phenomenological observations designed to give information suited for use in continuum mechanics theories. Such an approach is not sufficient if one wants to explain the inelastic behavior under load levels sufficient enough to initiate cracking and other forms of damage in the material. Their analysis can predict with high accuracy for small deformation and behavior. However, the continuum mechanics formulation may have some limitations when it is used to investigate initiating cracks or other forms of material damages; elements may undergo large deformations and may detach from other elements. This is because those approaches seldom cover the behavior of discrete, disjoint materials in detail.

Fracture mechanics was first studied for brittle materials such as glass by Griffith (1920). After about forty years, the concepts of fracture mechanics were applied to cementitious materials. The first applications to concrete appear to have been made by Neville (1959) and by Kaplan (1961). A historical review and an annotated bibliography of the application of fracture mechanics to cement and concrete was given by Mindess (1983). The application of fracture mechanics to concrete structures has provided new ways of understanding and modeling phenomena which could only be treated empirically before. In recent published literature, some works covering the main parts of development have been presented by Wittman (1983, 1986), Bazant (1985, 1986), Shah (1985), Carpinteri and Ingraffea (1984), Sih and Ditommaso (1985), Reinhardt (1986), Carpinteri (1986), Bazant (1992), Mihashi *et al.* (1993), and by Bazant *et al.* (1994).

A new discrete element approach has been needed for models based on micromechanical characterizations of inter-particle contact properties, which includes friction, normal stiffness, and tangential stiffness. Discrete element methods (DEMs) are numerical techniques designed specifically for simulating the complete behavior of a discontinuous material, and to solve problems in disconnected, partially connected, or fully connected structural assemblies. For example, the DEM can be applied to analyze interacting rigid or deformable bodies undergoing large dynamic or pseudo static motion, governed by complex constitutive behavior.

The discrete element approach has been developed over the last three decades to represent the behavior of cohesionless granular materials (Cundall 1971, Cundall 1974, Cundall and Strack 1979). It has since been modified and improved by a number of researchers to include applications such as deformation of sand, snow, pack ice, ceramic powder, blasting, and fluid mechanics (Rothenburg 1980, Bathurst 1985, Nelson and Issa 1989, Bruno and Nelson 1991, Van Baars 1996, Tran and Nelson 1996). Zubelewicz and Mroz (1983) and Zubelewicz and Bazant (1987) used a micro-mechanical approach to model concrete fractures. In the discrete element method, the system consists of discrete, disjoint interacting particles that are free to move except during contact with neighboring objects. Particles can undergo large displacements and large rotations, and they are typically used to model failure of weakly connected discrete systems under high loads. The equation of motion for each individual particle relates all contact and body forces to the particle mass, acceleration, and the inertial damping coefficients. The particle movement and mechanical interaction are tracked over time with an explicit central difference technique (Bathe and Wilson 1976). The contact forces in the microstructual level are then related to macroscopic boundary stresses through the principal of virtual work (Bathurst and Rothenburg 1990).

In the present study, the discrete element approach is used to simulate the response of materials up to the point of complete failure by modeling the intergranular deformation between aggregates

and bond cementation. Bond cementation, which is composed by a series of spring elements, attaches to the edges of the aggregate cores. Thus, the material response is simulated by a two-phase mortar aggregate composite (Rhie 1996, Rhie and Tran 1998, Tran *et al*. 1998). This can be accomplished by representing the material as an assembly of two dimensional (2D) polygon blocks, where each block is made up by a rigid aggregate center and a deformable cement paste enclosing the rigid core. A realistic quasi-brittle material response is achieved by combining the discrete element method - to model arbitrary motion of a large assembly of objects - with a Mohr-Coulomb fracture limit for the spring elements interconnecting the edges of neighboring aggregate particles. It helps to develop an improved understanding of the process of fractures or crack propagations, and to develop a realistic and simplified non-continuum model to simulate failure in this quasi-brittle material.

2. Discrete element formulation and implementation

2.1 General concept of modeling and algorithm

In setting up a discrete element model, the first major decision is whether or not to use two dimensional (2D) or three dimensional (3D) models. If the decision is to use 3D models, the only computationally practical shape of the particles, which can be treated for large systems of variable sized particles, are spheres. These types of systems can be used to study a number of processes. But assemblies of spheres are unstable unless subjected to external confinement. This is not the case for real geologic assemblies (e.g. piles of stones). The shape of the individual components of the aggregate is an important effect which is not accounted for when using spheres. If 3D objects other than spheres are considered, the computational burden becomes overwhelming even for small models. If, for example, a 200×200 2D array of objects appears on the faces of a cubical 3D assembly, on that face 4×10^4 blocks may be seen. But actually more than $(200)^3 = 8 \times 10^6$ objects will be needed to make up the 3D assembly, in fact, 1×10^7 3D objects. The object therefore must have an extremely simple shape and obey extremely simple physical contact rules if any hope exists for analysis of the assembly. If a 2D model is used, the individual objects making up the discrete element assembly (say our 200×200 model, with 4×10^4 blocks) can be assigned a variety of shapes from round (disks) to arbitrary polygonal. The 2D disk model is simplest, but suffers from the same problems described for 3D sphere assemblies. The 2D polygons can be used to investigate a large number of different shapes, sizes, and orientation effects of blocks. It is more costly to perform this because the contact logic between large numbers of polygons has been prohibitive until recently. Now it is the preferred 2D type of block or basic element. Of course, a 2D model has many limitations, the main one being that crack growth is 3D and the growth around blocks may not be as realistic as a 3D model could treat. Also, interstitial filling and void are not effectively captured with 2D models. Thus, in this study, we are going to adopt a model based on assemblies of 2D polygonal objects. Even then, very significant computer costs will occur, especially when complete physical modeling is required.

The important aspects of any discrete element program are the representation of contacts, the representation of solid material, and the scheme used to detect and revise the set of contacts between the discrete objects or blocks making up the assembly. Contact logic is surprisingly complex even for 2D blocks (circular disks or polygons), especially under the general motion and

when blocks of significantly different sizes are being considered. This is often one of the most time consuming parts of discrete element analysis. But a more difficult problem is defining a general and reliable contact force logic, especially when it involves a combination of normal and shear force effects. On top of this problem is the problem of effectively treating the initiation and evolution of cracking between blocks.

Concrete is a heterogeneous material made up by a finite-sized randomly distributed aggregate embedded in finer bond cementation and a number of voids. This multiphase material is approximated by a two-phase cementation-aggregate composite, in which the aggregate cross sections are modeled as random shaped polygons with different sizes. The shape of the individual aggregate components has an important effect on the mechanical behavior, and it needs to be accounted for.

Several algorithms are known to generate randomly shaped polygons in different sizes. Voronoi polygons (Finney 1979) divide the plane into an assembly of regions whose boundaries are the perpendicular bisectors of the lines joining the point pair of the nearest neighboring data points. To generate somewhat simpler and more realistic shaped aggregate particles, a procedure based on the Delaunay triangulation method is used (Delaunay 1934). This formulation is based upon a single observation that three given points will form a Delaunay triangle if the circumcircle defined by these nodes contains no other points. From the set of all possible triangles, the Delaunay method rejects the triangles with non-empty associated circumcicles. The algorithm was modified by Watson (1981), Sloan (1987), Cline and Renka (1984) to get an improved and more efficient formulation. Polygon shaped regions are then obtained from the given triangles by connecting the midpoints of those triangles connected at the vertex, see Fig. 1.

The geometric layout of the mortar-aggregate composite is generated by shrinking the size of the original polygons such that the rigid aggregate takes up to seventy five percent of the block and the remaining twenty five percent representing the cement paste matrix. In this idealization, two opposite-facing edges of neighboring polygon aggregates always exist, and they are connected by a deformable cement interface (Fig. 2). The stiffness and constitutive law of the interface bond will determine the overall strength and crack propagation characteristics of the block.

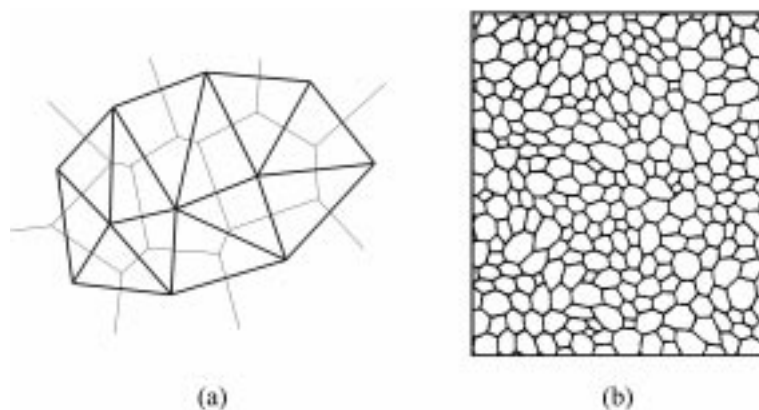(a)   (b)

Fig. 1 (a) Delaunay triangulation (bold line) and Voronoi diagram (fine line) (b) Assembly of Voronoi polygon particles
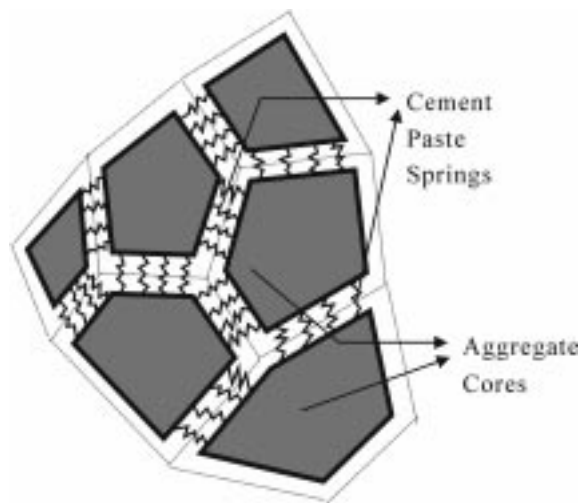
Fig. 2 Discrete element representation of cement-aggregate interaction

The cement properties are idealized and modeled as shown in Fig. 4. The physical mortar area enclosed by edges of neighboring aggregate particles is approximated by a rectangular shaped interface area; the interface area is modeled by equivalent non-linear spring elements. Depending on the force state, springs are either connected to the rigid polygons or separated from them. The separation occurs when the springs exceed a given limit state. Thus, the analysis must be able to distinguish and select between two possible states. First, the assembly behaves as a complete, connected system, and it is considered a continuum media. By increasing the applied load, some of the links will fail and the assembly will start to generate microcracks accompanied by a reduction in the overall strength of the material. Second, as the cracks propagate, fewer links exist to transfer the applied loads, aggregate particles will eventually be completely separated, and the analysis will be carried out following the discrete element logic. In this second state, the system consists of discrete, disjoint interacting particles, free to move except during contact with neighboring objects. Intergranular contact forces are determined by a discrete block logic where the magnitude depends on a contact detection law and an associated stiffness formulation. The flowchart for the main discrete element algorithm is shown in Fig. 3.

2.2 Formulation of connected blocks (Continuum state)

The discrete block should be connected to other similar blocks to simulate the behavior of a quasi-brittle material mass. Each polygon block is connected by four springs whose moduli are selected by experimental results. Actually each spring shown is two separate springs: a shear spring and a normal spring. Blocks (or polygon elements) start to move when forces are applied. Then the spring forces are produced.

The equivalent rectangular element interface is shown in Fig. 4(a). Consider the two rigid blocks A and B that share a common edge. P and Q are the two ends of this common edge. Aggregate core A is defined by vertices $A_1 - A_2 - A_3 - A_4 - A_5$, and aggregate core B is defined by vertices $B_1 - B_2 - B_3 - B_4$. The cement paste region C that is connecting the two blocks is defined by the
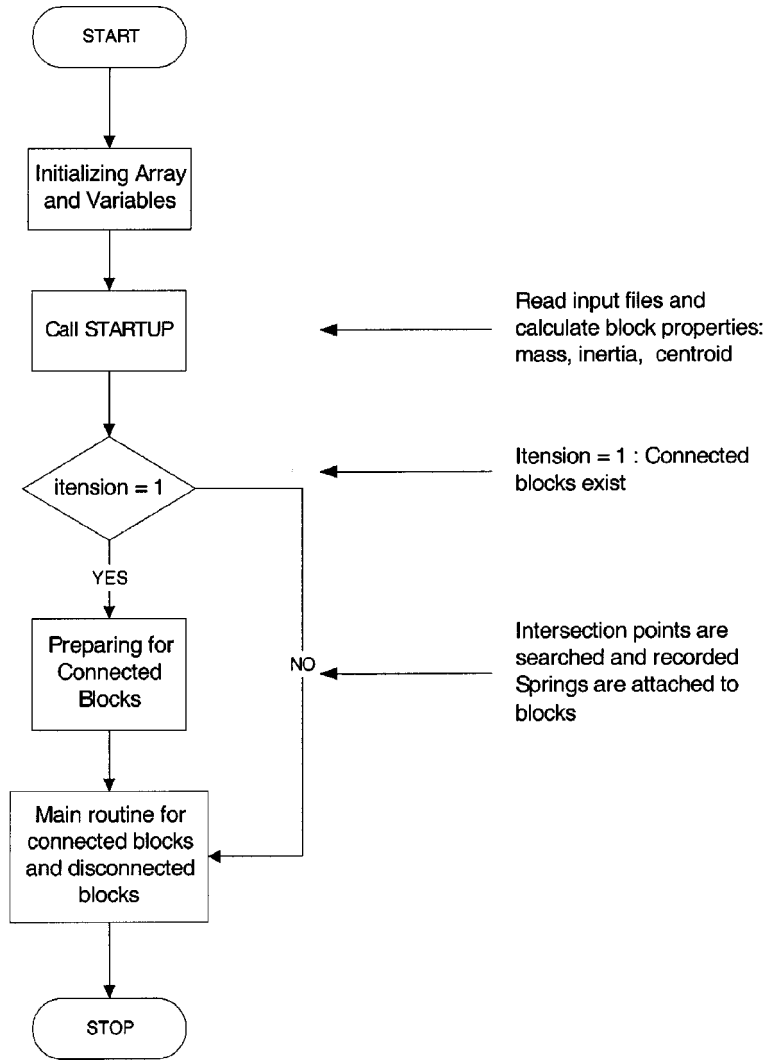
Fig. 3 The flowchart for the main discrete element algorithm

polygon $P - A_1 - A_2 - Q - B_2 - B_3$. This irregular cement paste region C is then transformed to a rectangular shape $A_1 - A_2 - B_2 - B_3$. That area is the same as that of C and is illustrated in Fig. 4(b). The new rectangular cement paste region is then subdivided into 4 equal rectangular shapes, with length L as the distance between the two parallel line segments A_1A_2 and B_2B_3, and width W as the length of the equivalent cement. Each small rectangular shape is modeled as a spring, and its normal stiffness (k_n) and shear stiffness (k_s) respectively can be calculated as follows:

$$k_n = \frac{E}{L}\left(\frac{W}{N}\right) \quad \text{and} \quad k_s = \frac{G}{L}\left(\frac{W}{N}\right) \tag{1}$$

where E is the Young Modulus, G is the shear modulus, N is the number of springs (i.e., $N = 4$), and L is the length of the rectangular shape. The shear direction for these four springs is defined as
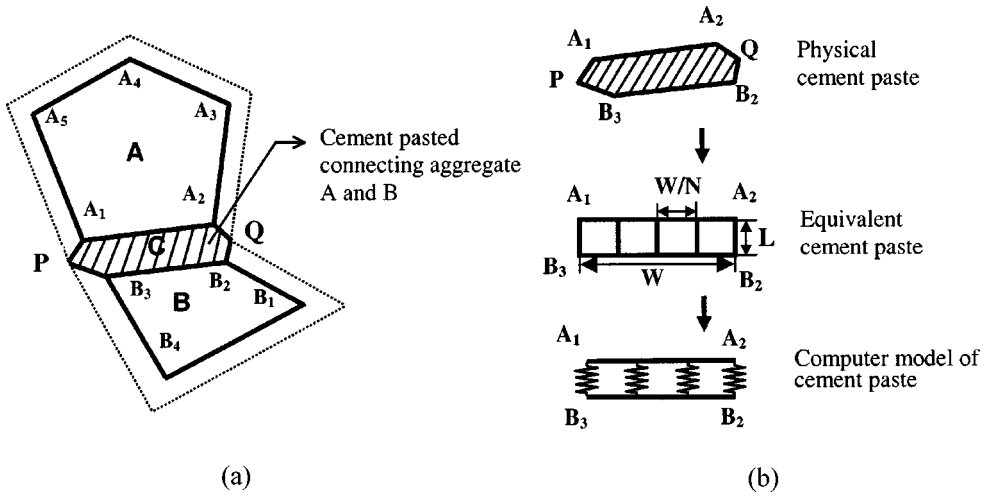
Fig. 4 DEM model of the cement paste between 2 rigid blocks

follows: The shear line of action is the line connecting the midpoint P of the line segment A_1B_3 and midpoint Q of line segment A_2B_2. The normal direction for the springs is the direction that is perpendicular to the shear line of action PQ. The normal and shear forces generated by the cement paste springs can be computed as:

$$F_n = \sum_{i=1}^{4} k_n \delta_n^i \quad \text{and} \quad F_s = \sum_{i=1}^{4} k_s \delta_s^i \tag{2}$$

where δ_n^i is the change in length in the normal direction of cement paste spring i, and δ_s^i is the change in length in the shear direction of the cement paste spring i.

The failure criterion, which has been found as the most widespread use for both rocks and concrete, is the Mohr-Coulomb criterion. The Coulomb internal friction theory is usually expressed in the form $\tau = C + \mu\sigma$, where C is the shear strength when $\sigma = 0$, and μ is the coefficient of internal friction. The Coulomb theory, in its original form, is applied only to compressive states of stress, in which failure was considered to occur in a shearing mode. There are two different types of failures in quasi-brittle materials such as concrete or sedimentary rocks: tensile or cleavage failure and compressive or shear failure. Compressive or shear failure is governed by the linear Coulomb equation, and the criterion for cleavage splitting is a limiting maximum tensile stress σ_t. The cement paste springs are assumed to deform in an elastic manner within limits of a bilinear failure of the Mohr-Coulomb criterion, illustrated in Fig. 5. In the Fig. 5, normal stress is plotted along the horizontal axis, and the shear stress is plotted on the vertical axis. The cement paste spring is defined to yield when the combination of shear and normal stress acting across the bond define a point on or above the solid failure lines shown. In our discrete element model, the two discrete blocks are connected by four springs. If one or more springs yield, the fracture process starts. When all four springs yield, a crack is formed between the two rigid aggregate blocks. The cement paste springs are permanently disabled after the forming of the crack, and the bond between the blocks is no longer holding them together.
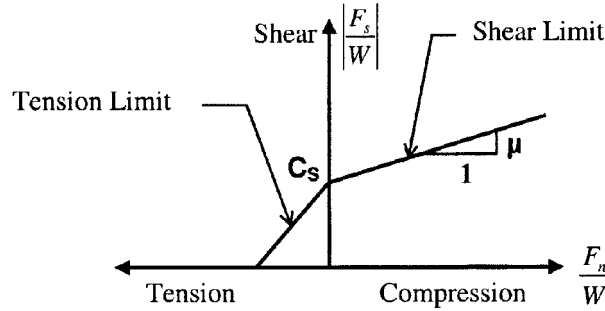
Fig. 5 Modified Mohr-Coulomb failure model for interface bonding

The Mohr-Coulomb equation for each cement paste spring is defined as:

$$\left| \frac{F_s}{W} \right| > C_s + \mu \frac{F_n}{W} \tag{3}$$

where F_s is the maximum resistant shear force between aggregates in the tangential direction, C_s is the cohesive constant, μ is the friction coefficient, and F_n is the normal force acting between elements. Once a fracture occurs, then C_s and μ both tend towards zero. The cohesion and friction coefficients may decrease with each increasing slip displacement. As the number of springs connected to aggregate blocks increase, the abrupt detachment effects of the blocks will be reduced.

2.3 Formulation of disconnected blocks (Discrete state)

Being the preparing step for the disconnected block logic, the contact detection logic should be executed first. This logic is a basic and complex procedure in the DEM. The contact logic procedure is the most costly and time consuming part of the analysis. The contact detection process uses a box-based logic where every 2D polygon is circumscribed by a rectangular box. The scheme for the contact detection consists of three level checks. In the first level, the check is performed to determine whether any two rectangular circumscribing boxes are in contact. In the second level, if the two boxes are in contact, the check is performed to eliminate cases in which the two polygons are not in contact, despite the contact of boxes. If the second level check shows that contact might occur, the third level check is performed to determine whether contact has in fact occurred (Tran and Nelson 1996).

Even if complete information regarding the interference between two blocks - including the block velocities in the region of the interference - is given, the contact shear and normal force directions are far from obvious, and the interaction between these forces is not fully understood. Tran and Nelson (1996) suggested "reasonable" definitions of the contact forces. They tested several examples, which are triaxial compression tests, dynamic analysis of hopper granular flows, etc., by using discrete block models. The results were reasonable and not far from realistic. This logic plays an important role in the present approach to modeling the behavior of quasi-brittle materials under several applied loadings.

To derive reasonable mathematical definitions of the contact forces, the velocity of the centroid of each block in the contact region is needed. The relative velocity, i.e. the difference in velocity of the

centroid of the contact area in block A and the velocity in block B, gives some sense of relative motion of the blocks.

The normal contact force is assumed to be independent on the contact area while the shear force is assumed to depend on both the contact area and the relative velocity of the centroids of the bodies in the contact zone, as well as the frictional properties between the two bodies.

Let the two intersection points be intersection point $P_1(x_1, y_1)$ and intersection point $P_2(x_2, y_2)$. The line connecting these two points is the line of action of the shear force. This line is represented by the vector S

$$S = (x_1 - x_2)\boldsymbol{i} + (y_1 - y_2)\boldsymbol{j} \tag{4}$$

During the sliding, the magnitude of the shear force is to be proportional to the area of the contact. However, the contact area alone is inadequate in defining the shear force. To illustrate this, consider two blocks approaching each other with the same speed but in opposite directions. When they are in contact, only normal contact force exists. In this case, the contact area is not zero, but the shear force equals zero. Thus, the shear force must depend on not only the contact area but also the differential motion of the two blocks. In the current formation, a relative velocity between the centroids of the overlapping regions of the blocks in contact is defined to formulate the contact shear force. This velocity is the velocity of the centroid of the contact region of one block as seen from a reference frame fixed at the same point in the other block. The relative velocity of the contact centroid is defined below. The velocity in polygon A is

$$\boldsymbol{V}^A_{cg_{contact}} = \boldsymbol{V}^A + \boldsymbol{\varpi}^A \otimes \boldsymbol{r}^A \tag{5}$$

and polygon B is

$$\boldsymbol{V}^B_{cg_{contact}} = \boldsymbol{V}^B + \boldsymbol{\varpi}^B \otimes \boldsymbol{r}^B \tag{6}$$

where, $\boldsymbol{\varpi}^A$ and $\boldsymbol{\varpi}^B$ are the angular velocities of blocks A and B, and $\boldsymbol{r}^A$ and $\boldsymbol{r}^B$ are the distances between the contact centroid and the centroids of blocks A and B.

The velocity of A relative to B at the centroid of the contact area may then be computed by subtracting the velocity of block B from the velocity of block A

$$\boldsymbol{V}^{\text{rel}}_{cg_{contact}} = \boldsymbol{V}^A_{cg_{contact}} - \boldsymbol{V}^B_{cg_{contact}} \tag{7}$$

A unit vector in the direction of the relative velocity is determined.

$$\boldsymbol{U}_{V^{\text{rel}}_{cg}} = \frac{\boldsymbol{V}^{\text{rel}}_{cg}}{\left|\boldsymbol{V}^{\text{rel}}_{cg}\right|} \tag{8}$$

Once this unit vector is found, its projection on the unit vector defining the direction of shear force (the cosine of the angle formed by these two vectors) will determine the fraction of the relative velocity that will be used in the shear force calculation.

Then, the shear force F_s is defined as

$$\boldsymbol{F}_s \; = \; (A * k_n * \mu_k * \boldsymbol{U}_{v_{cg}^{rel}} \cdot \boldsymbol{U}_s) \boldsymbol{U}_s \tag{9}$$

where $\boldsymbol{U}_s$ = unit vector in the direction of the shear, μ_k = dynamic coefficient of friction between the polygons, A = overlapping contact area, and k_n = constant proportional factor to be used in defining the normal force between the two polygons in contact.

The normal force is perpendicular to the shear force and can be easily found. It should be noted that the normal force is always compressive; therefore, the compressive normal force acting on a given polygon always points towards the body of the polygon such that, i.e., the force and the vector from the centroid of the interface area to the centroid of the polygon form an acute angle. Let the normal force vector unit be $\boldsymbol{n}$. The simplest normal contact force law may be written as

$$\boldsymbol{F}_n \; = \; A k_n \boldsymbol{n} \tag{10}$$

It is noted that this normal contact force logic has a linear relationship between the contact force and the contact area for both the unloading and loading stages.

The contact forces are constructed differently in the loading and unloading stages by changing the relationship between the normal contact force and the contact area. During the loading, the normal contact force is taken to be a quadratic function of the overlapping contact area. Upon unloading, the contact force is taken to be a linear function of the contact area where the slope depends on the past history of loading. The contact normal forces between the discrete rigid blocks in the loading stage are related to the contact area as follows.

$$F_n^l \; = \; F_{res} + a_1 A + a_2 A^2 \quad \text{with} \quad F_{res} = \sum_{i=1}^{4} F_n^i \tag{11}$$

When the blocks are in the unloading stage, the contact normal force is computed as shown below

$$F_n^u \; = \; F_n^{\max} - K(A_{\max} - A) \frac{dF_n^l}{dA}\bigg|_{A_{\max}} \tag{12}$$

where $A_{\max}$ = maximum overlapping contact area, $F_n^{\max}$ = maximum normal contact force, a_1 and a_2 = input parameters describing the nonlinear force relationship, K = parameter controlling the unloading rate of the linear force relationship, $dF_n^l/dA\big|_{A_{\max}}$ = derivative of the loading curve with respect to A evaluated at $A_{\max}$, F_n^i is the normal force of cement paste spring i, and F_{res} is the sum of the spring yielded forces carried over to the contact force to avoid a jump in the contact force.

The contact shear force between two polygons in the loading and unloading stages is taken to be proportional to the contact normal force

$$F_s \; = \; \mu_k F_n \tag{13}$$

where μ_k is the dynamic coefficient of the friction between the polygons. The dynamic coefficient is needed to get contact forces which depend on the relative velocity of the centroid of each block in the contact region. The difference in velocity of the centroid of the contact area of the two blocks gives some sense of relative motion of the blocks.
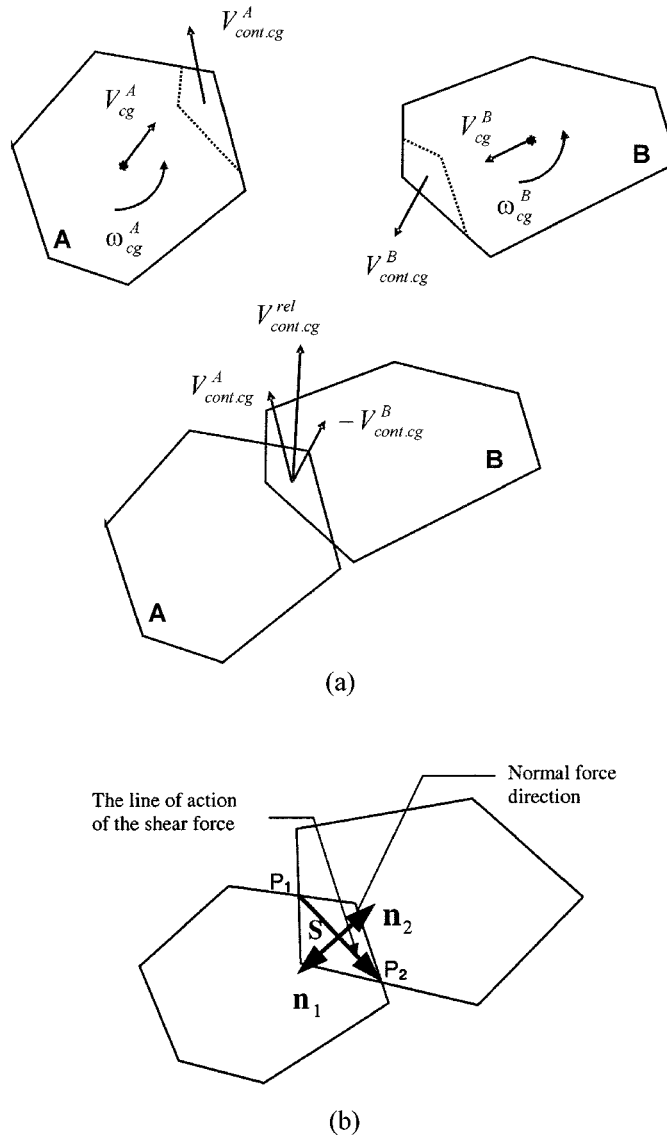
(a)

(b)

Fig. 6 (a) Direction of relative block velocities (b) Shear force line of action and normal force direction for disconnected blocks

3. Equation of motion

Each rigid block element, having mass M and moment inertia I, is assigned three independent degrees of freedom at its centroid: namely U_x, U_y, the displacements in the x and y directions, and Θ, the rotation about the z axis. The equations of motion of each block can be written as

$$M \ddot{U}_\alpha + C \dot{U}_\alpha = F_\alpha \qquad (\alpha = x, y) \tag{14}$$

$$I\ddot{\Theta} + D\dot{\Theta} \;=\; T \tag{15}$$

where F_α is the sum of all forces acting on the element in α direction, and T is the sum of all moments acting on it about its centroid. C and D are (inertial) damping coefficients. U_α is the displacement, and Θ is the angular displacement. Eqs. (14) and (15) can be solved using a direct time marching algorithm, such as the explicit central difference method (Bathe and Wilson 1976). Assuming that the displacement, velocity, and acceleration vectors at time Δt - denoted by $U_\alpha^{\Delta t}$, $\dot{U}_\alpha^{\Delta t}$, and $\ddot{U}_\alpha^{\Delta t}$ respectively - are known, then in this time integration scheme, the solution is advanced to times $k\Delta t$, $k = 2, 3, \ldots$ to solve for all times from 0 to T. In other words, the method establishes an approximate solution at times $0, \Delta t, 2\Delta t, 3\Delta t, \ldots, T$.

The critical stability limit, which is known as Courant's stability limit on Δt, is $\Delta t_{cr} = T_{cr}/\pi$. Actually this critical time step is only an estimate for two reasons. First, the stiffness K depends on the number of blocks in contact, which may be very hard to predict for an entire solution over an extended time. Second, the contact forces which make up F and T are higher nonlinear functions of block motion. If the blocks are permitted to move too far in any one time step (even if $\Delta t < \Delta t_{cr}$), the new positions of the block may generate extremely large forces and cause the assembly of blocks to appear to blow up. In practical numerical computations, control of the time step size is complicated, yet it is an important aspect of the numerical analysis.

4. Applications

4.1 Numerical input parameters

To simulate the sample concrete models shown in this study, numerical input parameters for the cement paste are used as follows; Young's modulus is 20,700 MPa (3×10^6 psi), Poisson ratio is 0.25, the bond tension limit is 6.9 MPa (1×10^3 psi), and the bond shear limit is 13.8 MPa (2×10^3 psi) (Newman *et al*. 1969). The parameters for the discrete contact force relationships for the aggregates are applied to simple primitive models in soil mechanics. The values of a_1, a_2, K and μ_k used in these tests are 20,700 MPa (3×10^6 psi), 20,700 GPa (3×10^9 psi), 2.5, and 0.3 respectively (Tran 1993).

4.2 Compressive failure simulation

Compression strength is the major criterion when assessing the quality of concrete-like quasi-brittle materials. Knowledge of the compression strength means that we have fairly accurate ideas about its strength when subjected to other loads, as well as its other mechanical properties. The methods applied throughout the world to assess the compression strength of concrete are similar. The differences consist only in shapes and sizes of the test specimen used, which can be cubes, cylinders, or prisms of various sizes. The testing technique in a laboratory is very important because friction between the specimen, the loading machine plates, and the quality of the contact between the two active surfaces - as well as the loading rate - greatly affect the test results. The numerical tests performed must recognize the effect of friction and the loading rates.

A rectangular shaped specimen model shown in Fig. 8(a) represents the prismatic or cylindrical specimen. The model shown in Fig. 8(b) is made of an assembly of 626 aggregate particles, and the
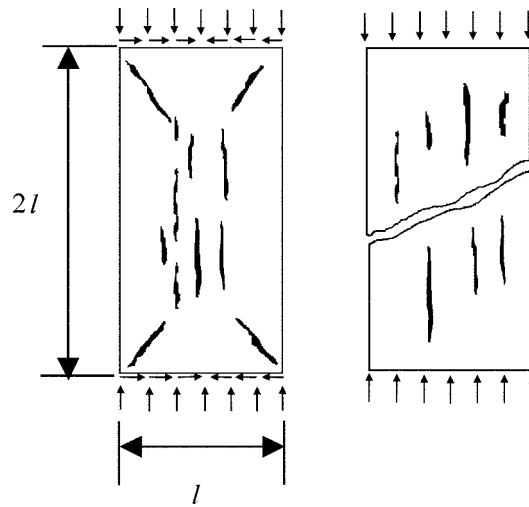
Fig. 7 Fracture patterns for rectangular and square specimens under compression of concrete-like material

geometric dimensions are a height of 30 cm and a width equal to 15 cm. The shapes of the 626 particle elements vary between 3 to 9 nodes for the rectangular specimen. The specimen is placed between two moving end platens to apply a constant strain rate loading. Friction between contacting surfaces generate shear stress components and induce a lateral confinement to the test specimen. For the non-lubricated specimen, cracks propagate parallel to the loading direction in the central zone of the specimen and slanting at the ends as the results of the shear force which is induced by platen friction. This state of stress generates a failure mode which is different from the ones with lubricated end platen as shown in Fig. 7 (Avram *et al*. 1981). Regardless of the specimen size, the ultimate compressive strength value of the lubricated specimen is slightly lower than the case of the non-lubricated specimen.

   The top block is moves down gradually over time to apply the compressive strain. In these numerical tests, three different end conditions are considered. The first assumes lubricated end faces with zero friction. In the second model, friction exists between contacting surfaces. And finally, in the last model, the end faces are not allowed to expand in the lateral direction. Fig. 8(b) shows the compressive failure mode of the specimen without friction. Cracks develop parallel to the applied load. In Fig. 9(a), friction exists between end faces and loading platens. Crack propagation occurs to form typical failure cones. The failure process, with fully constraint end faces, is shown in Fig. 9(b). The failure mode is again influenced by the boundary conditions at the top and bottom faces of the specimen.

   Numerical tests have been performed with three different heights specimens. The heights of the compressive specimens are 50 mm, 100 mm, and 200 mm. All specimens' widths are the same, 50 mm. Specimens with different heights have almost identical stress-strain behavior up to the peak stress. However, longer specimens exhibit less strain after the peak stress compared to shorter specimens (Fig. 10a), i.e., the softening part of the compressive stress-strain curves depends on the length of the specimens. The numerical results indicate that post-peak compressive stress-strain curves depend on the height of prismatic specimens. In Fig. 10(b), the stress-displacement curves show similar values for the post-peak behavior. The numerical results match well with Van Mier's (1986) experimental results for the plain concrete.
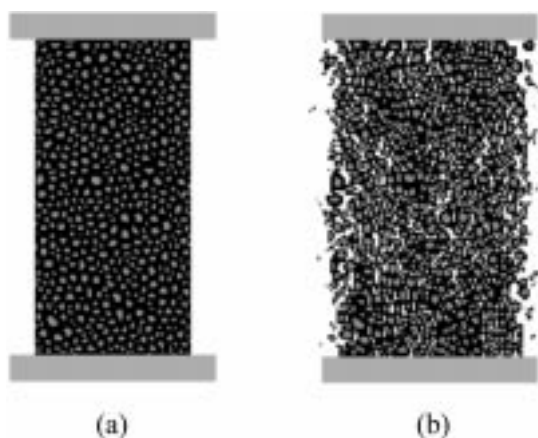
Fig. 8 (a) Compression specimen with rigid end platens (b) Fracture propagation of compressive specimen with lubricated end platens
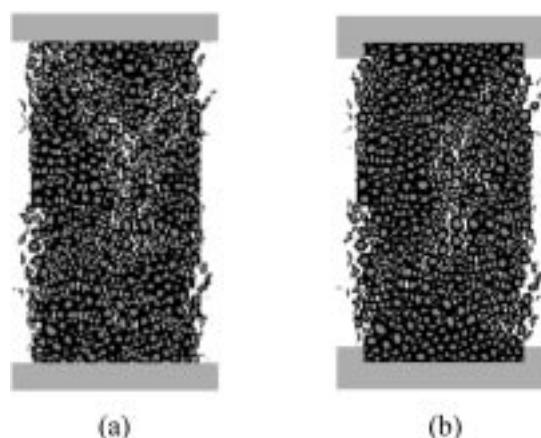
Fig. 9 (a) Fracture propagation of compressive specimen with non-lubricated end platens (b) Fracture propagation of compressive specimen with fully lateral constraint top and bottom face
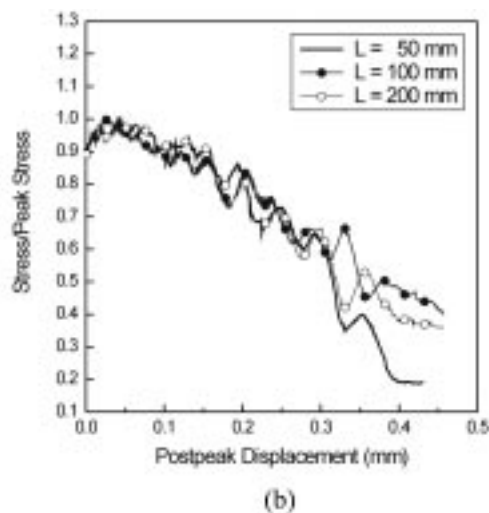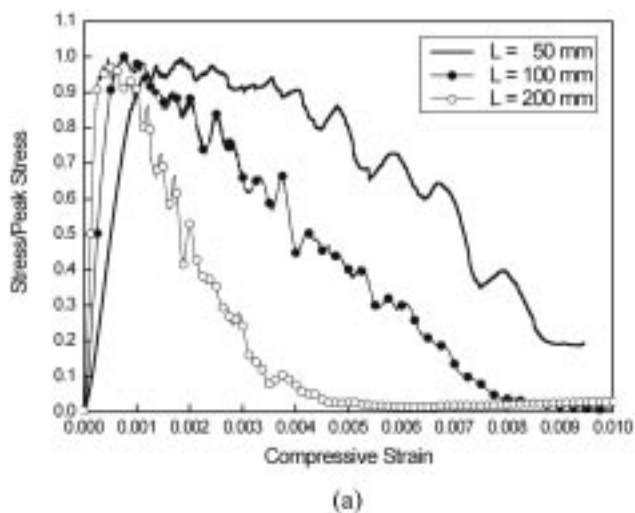

Fig. 10 Compressive response of prism models: (a) stress-strain relation (b) postpeak stress-displacement curves (Where, L = Length of Specimen, Width of Specimen = 100 mm)

4.3 Tensile failure simulation

Concrete material strength and limit strains under tensile stresses are essential parameters to be considered by the structural engineer confronted with practical or theoretical problems such as crack initiation and development, behavior to major stresses, torsion, etc. Although the strength under tension is of high practical interests, there are some difficulties in the test of specimens under
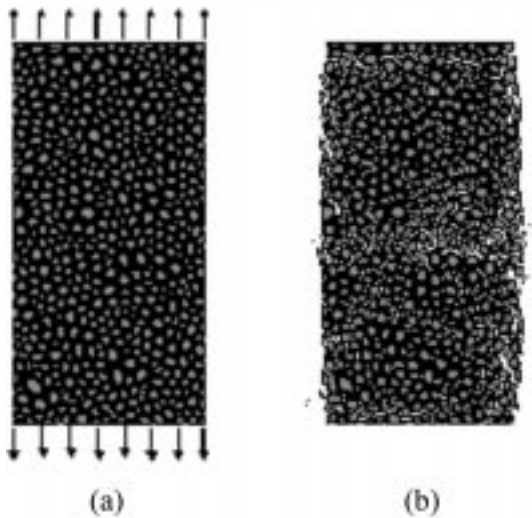
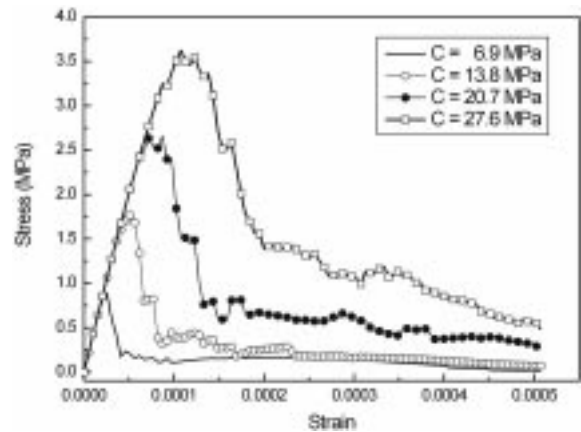Fig. 11 (a) Direct tension specimen (b) Crack propagation in direct tension

Fig. 12 Tensile stress-strain curves, corresponding to the function of cohesions

tension, namely the manner in which the samples have to be fastened between the jaws of the testing machine. Also it is not easy to obtain an even stress distribution over the cross section, because the stress field is disturbed by the specimen holding devices which introduce secondary stresses. By those reasons, direct tension tests of quasi-brittle materials are seldom carried out. To avoid all secondary effects and to obtain reliable results, the tests should be well instrumented and carefully executed.

Fig. 11 illustrates the overall response of the specimen subjected to direct tension. The failure process is a complex interaction and redistribution of the load carrying aggregate-cement components. Experimental evidence shows that the elastic limit is around 60 to 75% of the ultimate tensile strength. For higher stress levels, microcracking starts in the aggregate-cement interfaces, and the interval of stable crack propagation is usually very short. Upon further loading, active cracking zones develop suddenly and an unstable propagation is occurred normally to the loading direction. Thus, the behavior of concrete material in tension can be described as brittle in nature. Ultimately, the specimen separates from the loading near the top and bottom face. The stress-strain response of the tension specimen, as a function of different cohesive constants, is shown in Fig. 12.

5. Conclusions

The basic concepts of using the discrete polygon element models to investigate quasi-brittle materials have been explored. The contact logic between contacting, or nearly contacting, blocks has been checked and is believed to be sound. It is essentially Tran's logic, and a new connected block logic is added and improved.

The force logic has only just begun. In that, the force definition has been exercised to work through some basic examples with tracking the blocks by integrating their equations of motion. Results for compression and tension tests appear to be realistic, and they demonstrate many of the

characteristics of quasi-brittle material fracture and failure that have been observed in the laboratory.

A host of modeling options still exist which should be explored. In particular,

1) The logic of post crack behavior has many possible options which should be considered, such as the rate of loss of cohesion and friction coefficient, shear induced volume expansion, etc.

2) The size or type of the process zone, now believed to be of the order of the aggregate, needs to be investigated. It appears to be rather large in the current numerical results. A larger numerical model may be required.

The size and scope of the block model has, in the past, presented computational problems, especially when many comparative studies are being done. The nature of explicit, conditionally stable direct time integration means that quasi-static loading is an expensive numerical exercise. If the models, which are needed, become too large to be handled in general, special techniques to minimize the computational burden will have to be developed. For example, it may be necessary to limit the needs for updating contacts between aggregate and cement paste to only certain zones where cracks are actively forming, or for control of the model which has a huge amount of elements. Parallel processing techniques will be useful. Also, to use this scheme in practical areas, parameters of the equations that are defined in this paper should be studied and adjusted more in the future. Parameter studies will require a lot of time consuming procedures.

The DEM is a very interesting technique for exploring the nonlinear, inelastic behavior of random multiphase engineering materials. It is believed to hold real promise for integrating the basic mechanical behavior without relying heavily or phenomenological (experimental) test results.

Acknowledgements

References

Avram, Constantin, *et al.* (1981), *Concrete and Strength and Materials*, Elsevier/North-Holland, N.Y.

Bathe, K.J. and Wilson, E.L. (1976), *Numerical Methods in Finite Element Method*, Prentice Hall Inc., Englewood Cliffs, N.J.

Bathurst, R.J. (1985), "A study of stress and anisotropy in idealized granular assemblies", Ph.D. Dissertation, Queen's University, Canada.

Bathurst, R.J. and Rothenburg, L. (1990), "Observation on stress-force-fabric relationships in idealized granular materials", *Mech. of Mat.*, **9**, 65-80.

Bazant, Z.P. (editor) (1985), *Mechanics of Geomatrials*. Wiley, N.Y.

Bazant, Z.P. (1986), "Mechanics of distributed cracking", *Applied Mechanics Reviews*, **39**(5), 675-705.

Bruno, M.S. and Nelson, R.B. (1991), "Microstructural analysis of the inelastic behavior of sedimentary rock", *Mech. of Mat.*, **12**, 95-118.

Carpinteri, A. (1986), *Mechanical Damage and Crack Growth in Concrete. Plastic Collapse to Brittle Failure*, Martinus Nijhoff.

Carpinteri, A. and Ingraffea, A.R. (editors) (1984), *Fracture Mechanics of Concrete: Material Characterization and Testing*. Martinus Nijhoff, The Hague.

Cline, A.K. and Renka, R.L. (1984), "A storage-efficient method for construction of a Thiessen triangulation", *Rocky Mountain Journal of Mathematics*, **14**(1), 119-139.

Cundall, P.A. (1971), "A computer model for simulation progressive, large-scale movements in polygon rock

systems", *Proc. of Int. Symp. on Rock Fracture*, Nancy, France: II-8.

Cundall, P.A. and Strack, O.D.L. (1979), "A discrete numerical model for granular assemblies", *Geotechnique*, **29**(1), 47-65.

Delaunay, B. (1934), "Sur la sphère vide", *Bull. Acad. Sci. USSR(VII), Classe Sci. Mat. Nat.*, 793-800.

Finney, J.L. (1979), "A procedure for the construction of Voronoi polyhedra", *J. Comp. Physics*, **32**, 137-143.

Griffith, A.A. (1920), "The phenomena of rupture and flow in solids", *Philosophical Transactions. A*, Royal Society of London, **22**, 163-198.

Kaplan, F.M. (1961), "Crack propagation and the fracture of concrete", *J. ACI*, **58**, 591-610.

Mihashi, M., Okamura, H. and Bazant, Z.P. (1993), "Size effect in concrete structures", *Proc. the Japan Concrete Institute International Workshop*, Sendai, Japan, October.

Mindess, S. (1983a), "The application of fracture mechanics to cement and concrete: A historical review", in *Fracture Mechanics of Concrete*, F.H. Wittman (ed.), Elsevier, Amsterdam, 1-30.

Mindess, S. (1983b), "The cracking and fracture of concrete: an annotated bibliography 1928-1981", in *Fracture Mechanics of Concrete*, F.H. Wittman (ed.), Elsevier, Amsterdam, 539-680.

Nelson, R.B. and Bruno, M.S. (1991), "Microstructural analysis of the inelastic behavior of sedimentary rock", *Mech. of Mat*., **12**, 95-118.

Nelson, R.B. and Issa, J.A. (1989), "Numerical analysis of micromechanical behavior of granular materials", *Proc. of 1st Conf. On Discrete Element Method*, Golden, Colorado.

Neville, A.M. (1959), "Some aspects of the strength of concrete", *Civil Engineering* (London), **54**, 1153-1156.

Newman, K. and Newman, J.B. (1969), "Failure theories and design criteria for plain concrete Structure", *Proc. of the Southampton 1969 Civil Engineering Materials Conference, Solid Mechanics and Engineering Design,* **Part 2**, 963-995.

Reinhardt, H.W. (1986), "The role of fracture mechanics in rational rules for concrete design", *IABSE PERIODICA*, No. 1, IABSE Surveys, S-34/86, February.

Rothenburg, L. (1980), "Micromechanics of idealized granular systems", Ph.D. Dissertation, Ottawa, Ontario, Canada.

Rhie, Y.B. (1996), "A discrete element structural model for fracture of plane concrete", Ph.D. Dissertation, University of California, Los Angeles.

Rhie, Y.B. and Tran, T.X. (1998), "Microstructural analysis of the fracture behavior of plane concrete by using discrete element method", *Proc. of 12th ASCE Engineering Mechanics Conference*, San Diego, California, USA.

Sih, G.C. and DiTommaso, A. (editors) (1985), *Fracture Mechanics of Concrete: Structural Application and Numerical Calculation.*, Matinus Nijhoff, Dordrecht.

Shah, S.P. (editor) (1985), *Application of Fracture Mechanics to Cementitious Composites*, NATO ASI Series, Series E, Applied Sciences(94), Martinus Nijhoff, The Hague.

Sloan, S.W. (1987), "A fast algorithm for constructing Delaunay triangulations in the plane", *Advances in Engineering Software*, **9**(1), 34-55.

Tran, T.X. (1993), "Analysis of disjoint 2D and 3D particle assemblies", Ph.D. Dissertation, University of California, Los Angeles.

Tran, T.X., Dorfmann, A. and Rhie, Y.B. (1998), "Micromechanical modeling of cracking and damage of concrete structures", *Proc. of the Euro-C Conference on Computational Modeling of Concrete Structures*, Badgatein, Austria.

Tran, T.X. and Neslon, R.B. (1996), "Analysis of disjoint two dimensional particle assemblies", *J. Engrg. Mech.*, ASCE, **122**(12), 1139-1148.

Van Baars, S. (1996), "Discrete element analysis of granular materials", Ph.D. Dissertation, Delft University, Nederlands.

Van Mier, J.G.M. (1986), "Multi axial strain-softening of concrete, Part I: Fracture", *Mat. and Struc.*, **19**(111), 179-190.

Watson, D.F. (1981), "Computing the n-dimensional Delaunay triangulation with application to Voronoi polytopes", *The Computer Journal*, **24**, 162-172.

Wittman, F.H. (editor) (1983), *Fracture Mechanics of Concrete*, Elsevier, Amsterdam.

Wittman, F.H. (editor) (1986), *Fracture Toughness and Fracture Energy of Concrete*, Elsevier, Amsterdam.

Zubelewicz, A. and Mroz, Z. (1983), "Numerical simulation of rock-burst processes treated as problems of dynamic instability", *Rock Mech. and Engrg.*, **16**, 253-274.

Zubelewicz, A. and Bazant, Z.P. (1987), "Interface element modeling of fracture in aggregate composites", *J. Engrg. Mech.*, ASCE, **113**(11), 1619-1630.

Notation

k_n	: normal stiffness
k_s	: shear stiffness
E	: Young's modulus
G	: shear modulus
L	: length of the rectangular shape
F_s	: resistant shear force between aggregates in the tangential direction
F_n	: resistant normal force between elements
δ_n^i	: change in length in the normal direction of cement paste spring i
δ_s^i	: change in length in the shear direction of the cement paste spring i
C_s	: cohesive constant
N	: number of springs attached for each faced element
$\mathbf{S}$	: the line of action of shears
$\mathbf{V}_{cg_{contact}}^A$	: velocity in polygon A
$\mathbf{V}_{cg_{contact}}^B$	: velocity in polygon B
ϖ^A	: angular velocity of block A
ϖ^B	: angular velocity of block B
$\mathbf{r}^A$	: distance between the contact centroid and the centroid of block A
$\mathbf{r}^B$	: distance between the contact centroid and the centroid of block B
$\mathbf{V}_{cg_{contact}}^{rel}$	: velocity of A relative to B at the centroid of the contact area
$\mathbf{U}_{V_{cg}^{rel}}$	: unit vector in the direction of the relative velocity
A_{max}	: maximum overlapping contact area
F_n^{max}	: maximum normal contact force
a_1, a_2	: input parameters describing the nonlinear force relationship
K	: parameter controlling the unloading rate of the linear force relationship
$dF_n^l/dA\big|_{A_{max}}$	: derivative of the loading curve with respect to A evaluated at A_{max},
F_n^i	: normal force of cement paste spring i
F_{res}	: sum of spring yielded forces carried over to the contact force
M	: mass of rigid block element
I	: moment inertia of rigid block element
U_x, U_y	: displacements in the x and y directions of block elements
Θ	: angular displacement of block elements about the z axis.
F_α	: sum of all the forces acting on the element in the α direction
T	: sum of all the moments acting on the block element about its centroid
C, D	: (inertial) damping coefficients
U_α	: displacement in α direction ($\alpha = x, y$)
$U_\alpha^{\Delta t}, \dot{U}_\alpha^{\Delta t}, \ddot{U}_\alpha^{\Delta t}$	: the displacement, velocity and acceleration vectors at time Δt
Δt_{cr}	: critical time step